

Effect of earth resistivity on evaluating the corrosion risks from AC interference to pipelines

1. Kenneth Lax (ken.lax@corroconsult.com)

Corroconsult UK Ltd, Telford, United Kingdom (Presenting author)

2. Charalambos A. Charalambous (cchara@ucy.ac.cy)

University of Cyprus, Nicosia, Cyprus

3. David Boteler (david.boteler@canada.ca)

Natural Resources Canada, Ottawa, Canada

Abstract

Currents in power line conductors induce currents in nearby pipelines and in the earth beneath. The pipe-to-soil potential (PSP) variations produced by this AC interference depend on two factors:

- (1) the electromagnetic induction into the pipeline, and
- (2) the electrical response of the pipeline.

Evaluating Part 1 involves using information (amplitude, phase relationship and frequency) about the currents in the power line; the height of the power line and lateral distance to the pipeline; and the earth resistivity to calculate the electric field induced in the pipeline. This calculation can be done using Carson's formula or by using the complex image method.

Determining the pipeline response in Part 2 involves using the calculated electric field value as input to a transmission line model of the pipeline. This model involves the series impedance along the pipeline and the parallel admittance to ground. The admittance to ground is a function of both the coating conductance and resistivity of the soil surrounding the pipeline.

Thus, soil resistivity features in the calculations both in Part 1, dealing with electromagnetic induction, and in Part 2, dealing with the pipeline response.

The purpose of this paper is to examine the effect of different Earth resistivity values on AC interference to pipelines and to assess which resistivity values are important. Deeper resistivity values feature in the electromagnetic induction calculations of the electric fields, while the near-surface resistivity of the soil surrounding the pipeline features in the pipeline modelling. The conclusion is that the resistivity of the soil has no material impact on the calculations of the induced electric field and consequent pipe-to-soil potential (PSP) variations produced by the steady state AC interference.

Introduction

In many places, pipelines have been constructed to run along the same right-of-way as an AC power line. The AC currents in these power lines create varying magnetic fields that induce electric fields in the pipelines. This AC interference is one of the factors that needs to be considered when assessing and mitigating the corrosion risk for the pipeline.

Evaluating the pipeline interference involves two steps. Step 1 calculates the electromagnetic induction into the pipeline. Step 2 determines the electrical response of the pipeline.

Step 1 (calculating the electric field induced in the pipeline) involves:

- using information (amplitude, frequency, and phase relationship) about the currents in the power line
- the height of the power line and lateral distance to the pipeline
- the earth resistivity to calculate the electric field induced in the pipeline.

Step 2 (pipeline response to the induced electric field) involves:

- calculating the series impedance along the pipeline
- calculating the parallel admittance to ground, as a function of the coating conductance and the resistivity of the soil surrounding the pipeline.
- using the calculated electric field value as input to a transmission line model of the pipeline to determine the pipe-to-soil potential AC variations

Soil resistivity features in the calculations for both Step 1, dealing with electromagnetic induction, and Step 2, dealing with the pipeline response.

Deeper resistivity values are typically used in the electromagnetic induction calculations, while the near-surface resistivity of the soil surrounding the pipeline is usually included in determining the pipeline response. Thus, soil resistivity measurements are routinely made to provide data for the estimation of the corrosion risk to the pipeline and for the design of the cathodic protection anode groundbeds.

Soil resistivity and corrosion risk are discussed in various standards [1] [2] [3] [4]. Soil resistivity measurements are usually made using the Wenner 4 -pin technique, either directly in the soil or using a soil box. ASTM G57 [5] describes the measurement technique.

ISO 18086:2017 describes the impact of soil resistivity on the evaluation of the likelihood of AC corrosion. Clause 6.1.1 acknowledges that the “...*local soil composition and resistivity*” has a direct impact on the risk of corrosion damage. In Annex B it mentions using some of the excavated soil to measure the soil resistivity in a soil box. Annex D explains how the “*specific local soil resistivity*” influences the electrochemical corrosion process.

Cathodic protection anode groundbed and AC mitigation designs and corrosion risk evaluation rely on using the value of the soil resistivity at the proposed anode or pipe depth. Modelling software requires deep soil resistivity measurements.

One software modelling program requires 4-pin measurements of the soil resistivity at depths of 0.1 m to at least 200 m with 15 measurements at various intervals. The software requires measurements at:

- all exposed structures
- where powerlines deviate
- phase transpositions
- Crossings
- intervals of parallelism
- proximity to powerline structures
- proximity to grounding systems (including substations and power plants).

The purpose of this paper is to examine the effect of different Earth resistivity values on the calculations for Step 1 and Step 2 and to assess which resistivity values are important for assessing AC interference to pipelines.

We first explain the calculation of electromagnetic induction into pipelines and examine how earth resistivity values feature in the calculations. Then we present the pipeline modelling and show how earth resistivity values are used in these calculations.

Worked examples are presented to illustrate how the calculations can be made.

AC Induction in Pipelines

Calculation of the electromagnetic induction into a pipeline uses information (amplitude, phase relationship and frequency) about the currents in the power line, the height of the power line and lateral distance to the pipeline. These calculations are based on Carson's formulas [6] or simplified approximations such as the Carson-Clem formula [4] [7] [8] , or by using the Dubanton equations [9] also known as the complex image method (CIM) [10].

The process starts with the electric current in each phase of the power line. These currents create varying magnetic fields that induce electric currents in the Earth and these induced currents themselves create a varying magnetic field. Thus, the magnetic field variations seen by a pipeline at the Earth's surface are a combination of the "external" magnetic field variations produced by the power line currents and the "internal" magnetic field variations produced by the induced currents in the Earth.

Calculations of electromagnetic induction in pipelines need to take account of both the "external" and "internal" components of the magnetic field variations. Carson [6] first developed the theory for electromagnetic coupling between conductors at the Earth's surface and his formulas contain a correction term to account for the induced currents in the Earth. The full Carson's equations are complicated and various simplifying approximations have been suggested over the years. However, it has been shown that Carson's formulas can be accurately approximated by much simpler calculations using the complex image method [11].

The complex image method also has the advantage that it provides a simple visualisation of the “external” and “internal” contributions to the electromagnetic induction in a pipeline.

Complex Image Method

Induction in a pipeline at the Earth’s surface comprises external and internal components. The external part is the direct induction in the pipeline due to the magnetic fields from the currents in the power lines. The internal part is the contribution to induction in the pipeline from the magnetic fields due to currents induced in the Earth.

The magnetic fields produced by the induced currents in the Earth can be accurately represented by the magnetic fields produced by an image current at a complex depth. The complex depth depends on the height of the power line and the complex skin depth in the Earth. This is illustrated in Figure 1.

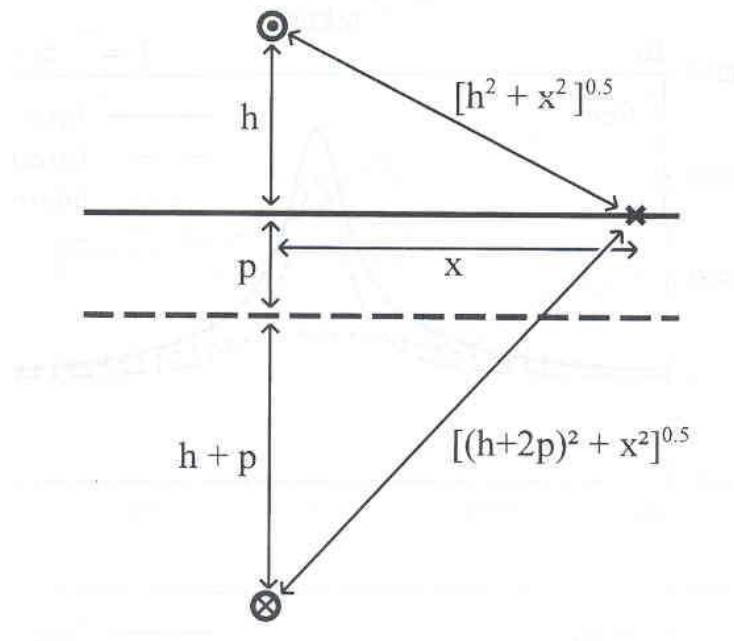


Figure 1 The complex image method. Calculations of the magnetic and electric fields at a point X on the Earth’s surface involves contributions from the external current at height, h, and an image current at a complex depth, h+2p.

Where:

h distance of the conductor above the surface (m)

x lateral distance from the pipeline (m)

h+2p complex skin depth

The magnetic fields produced by the currents can be resolved into two components: the horizontal field, B_x perpendicular to the power line, and the vertical field, B_z given by:

$$B_x = \frac{\mu_0 I}{2\pi} \left(\frac{h}{h^2+x^2} + \frac{h+2p}{(h+2p)^2+x^2} \right) \quad (1)$$

$$B_z = -\frac{\mu_0 I}{2\pi} \left(\frac{x}{h^2+x^2} + \frac{x}{(h+2p)^2+x^2} \right) \quad (2)$$

Where:

μ_0 permeability of free space (constant) (H.m⁻¹)

I current (A)

The induced electric field (E_y (V.m⁻¹)) parallel to the power line, at the position of the pipeline, is given by:

$$E_y = -if\mu_0 I \ln \left[\frac{\sqrt{(h+2p)^2+x^2}}{\sqrt{h^2+x^2}} \right] \quad (3)$$

Where:

f frequency (Hz)

The top and bottom of the ln term are the distance from the pipeline to the image current and the distance from the pipeline to the power line, respectively. The distance to the image current involves the complex skin depth, p , which can be obtained from the surface impedance Z_S , of the earth:

$$p = \frac{Z_S}{j2\pi f \mu_0} \quad (4)$$

The surface impedance depends on frequency and the resistivity structure of the Earth. Calculations are often made using the simplifying approximation of a uniform resistivity. However, calculations can also be made for the more realistic situation where resistivity varies with depth by modelling the earth as a series of layers with different resistivities (see Appendix).

For AC frequencies we need only consider the upper few kilometres of the Earth, but even within this thickness there can be significant differences between the resistivity of a surface soil layer and the resistivity of the underlying rocks. To examine how different values of resistivity and its variation with depth affect the complex skin depth we make calculations for 4 earth models:

- uniform earth models as shown in Figure 2 (a) with resistivity value of 10 ohm.m
- uniform earth with a resistivity of 100 ohm.m
- uniform earth with resistivity of 1000 ohm.m
- 2-layer earth model as shown in Figure 2 (b) featuring a surface layer with resistivity, $\rho_1 = 10$ ohm.m and an underlying uniform region with resistivity, $\rho_2 = 1000$ ohm.m.

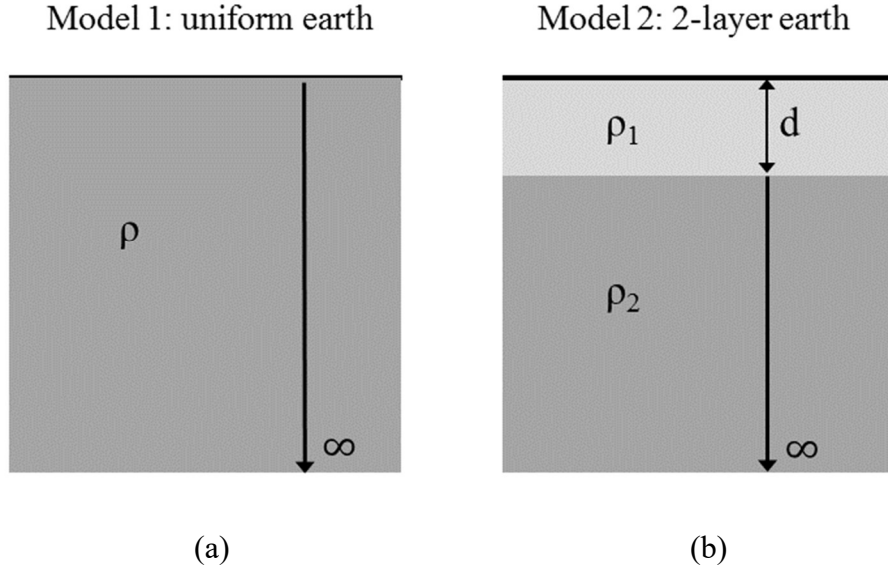


Figure 2 Earth models used in this study. Model 1 has uniform resistivity, ρ . Model 2 has a surface layer of depth, d , and resistivity, ρ_1 and an underlying region with resistivity, ρ_2

For a uniform resistivity, the surface impedance is given by:

$$Z_S = \sqrt{j2\pi f \mu_0 \rho} \quad (5)$$

Where:

j complex number ($\sqrt{-1}$)

ρ soil resistivity (ohm.m)

Substituting this into (4) gives the complex skin depth for a uniform resistivity model:

$$p = \sqrt{\frac{\rho}{j2\pi f \mu_0}} \quad (6)$$

For a 2-layer model, applying (A.19), the surface impedance is given by:

$$Z_S = \left(\frac{1 + R_2 e^{-2k_1 d_1}}{1 - R_2 e^{-2k_1 d_1}} \right) \eta_1 \quad (7)$$

Where k_1 is the propagation constant in the upper layer:

$$k_1 = \sqrt{\frac{j2\pi f \mu_0}{\rho_1}} \quad (8)$$

and R_2 is the reflection coefficient at the boundary between the top layer and the underlying region given by:

$$R_2 = \left(\frac{\eta_2 - \eta_1}{\eta_2 + \eta_1} \right) \quad (9)$$

In which η_n with $n= 1$ or 2 is the characteristic impedance of each layer:

$$\eta_n = \sqrt{j2\pi f \mu_0 \rho_n} \quad (10)$$

Substituting these into (9) and cancelling common terms gives

$$R_2 = \left(\frac{\sqrt{\rho_2} - \sqrt{\rho_1}}{\sqrt{\rho_2} + \sqrt{\rho_1}} \right) \quad (11)$$

This can be used in (7) to determine the surface impedance for the 2-layer model. This surface impedance can then be substituted into (4) to give the complex skin depth for the 2-layer model.

For the 2-layer earth model, the results depend on the thickness of the surface layer and the resistivity values. However, two limiting cases can be considered that provide some guidance of the results that can be expected.

For a surface layer that is thicker than the skin depth given by its resistivity value then $2k_1d_1 \gg 1$ and the exponential term $e^{-2k_1d_1} \rightarrow 0$ then the surface impedance can be simplified to

$$Z_S = \eta_1 \quad (12)$$

And inserting this into (4) gives

$$p = \sqrt{\frac{\rho_1}{j2\pi f \mu_0}} \quad (13)$$

Which is the complex skin depth that is obtained with a uniform resistivity with the value given by the resistivity of the surface layer. This shows the fields do not penetrate significantly into the lower layer, so the response is determined by the resistivity of the upper layer.

For a surface layer with thickness that is much less than the skin depth for the surface layer then $2k_1d_1 \ll 1$ and the exponential term $e^{-2k_1d_1} \approx 1$ and the surface impedance for the 2-layer model can be written

$$Z_S = \left(\frac{1 + R_2}{1 - R_2} \right) \eta_1 \quad (14)$$

Inserting into (4) gives the complex skin depth

$$p = \sqrt{\frac{\rho_1}{j2\pi f \mu_0}} \left(\frac{1 + R_2}{1 - R_2} \right) \quad (15)$$

Substituting for R_2 from (11), cross multiplying, and cancelling terms gives

$$p = \sqrt{\frac{\rho_1}{j2\pi f \mu_0}} \frac{\sqrt{\rho_2}}{\sqrt{\rho_1}} \quad (16)$$

Cancelling the $\sqrt{\rho_1}$ terms gives

$$p = \sqrt{\frac{\rho_2}{j2\pi f \mu_0}} \quad (17)$$

which is the complex skin depth for a uniform resistivity with the value given by the lower region in the 2-layer model. This shows that, in this case, the fields travel through the thin surface layer without being affected by it and the response is determined by the resistivity of the lower layer.

Thus, the results for a 2-layer model will be between the results for uniform earth models with resistivities given by the values for the top layer and the bottom layer.

For both the uniform earth and 2-layer models, once the complex skin depth has been calculated it can be used in equation (3) to calculate the electric field induced in a pipeline parallel to a power line.

Pipeline Modelling

To assess how the induced electric field affects the pipe-to-soil potentials of a pipeline, it is necessary to take account of the electrical properties of the pipeline. This is best done by modelling the pipeline as a transmission line with series impedance, Z , and parallel admittance, Y as shown in [13] [14]. The induced electric field is then represented by voltage sources distributed along the transmission line as shown in Figure 3.

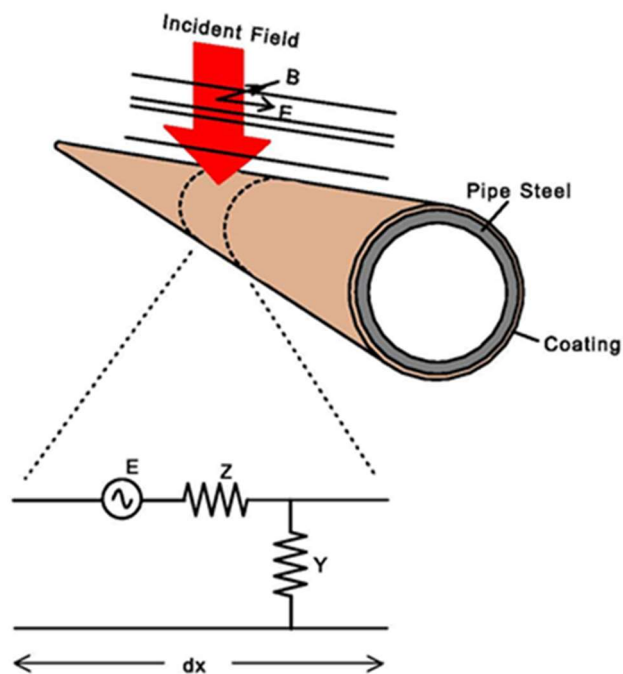


Figure 3 Schematic of electromagnetic induction in a pipeline and the equivalent circuit for a short pipeline section.

The series impedance and parallel admittance are used to give the propagation constant, γ , and the characteristic impedance, Z_0 , that describe the electrical response of the pipeline.

$$\gamma = \sqrt{ZY} \quad 18(a)$$

$$Z_0 = \sqrt{\frac{Z}{Y}} \quad 18(b)$$

The parallel admittance, Y depends on the conductance through the pipeline coating and the surrounding soil. Modern pipeline coatings have very high resistance (low conductance) that is much greater than the resistance of the surrounding soil, so the soil resistivity has little effect on the calculated value for the admittance, Y . The series impedance, Z , is determined by the steel resistivity and the pipe dimensions so is also not affected by the soil resistivity.

Thus, the derived parameters: pipeline propagation constant, γ , and characteristic impedance, Z_0 , are independent of the soil resistivity. A useful parameter for investigating the pipeline response is the inverse of the propagation constant which gives the distance over which the pipeline potential adjusts to changes in conditions, such as the end of the pipeline. For typical values of Z and Y at 50 Hz, the adjustment distance, $1/\gamma$ has values that are tens of kilometres.

Distributed-Source Transmission Line (DSTL) theory, as described in [14] allows electric fields that vary with distance along the pipeline and results in equations involving integrals of the electric field. For the example situation we are considering, the pipeline is parallel to the power line, so the induced electric field has the same value all along the pipeline. With a uniform value of the electric field, E , the DSTL equations simplify [13] and the pipeline potential can be written

$$V(y) = \frac{E}{\gamma} (Ae^{-\gamma y} + Be^{-\gamma(L-y)}) \quad (19)$$

Where A and B are constants dependent on the conditions at the end of the pipeline.

For pipeline lengths that are short compared to the adjustment distance, equation (19) can be simplified (see [13]) to give:

$$V(y) = E \left(y - L \frac{Z_1}{Z_1 + Z_2} \right) \quad (20)$$

Where:

- Z_1 and Z_2 impedances to ground at the ends of the pipeline (ohms)
- L length of pipeline (m)

If there are no groundbeds connected to the pipeline, then Z_1 and Z_2 should be set to the same high value, in which case they cancel and (20) reduces to:

$$V(y) = E (y - L/2) \quad (21)$$

In this case $V(y)$ varies from $-EL/2$ at one end ($y=0$) to $+EL/2$ at the other end ($y=L$) as shown in Figure 4.

Thus, the maximum pipe-to-soil potential produced by an induced electric field, E , on a short pipeline of length, L , is half the multiple of the electric field and the pipeline length.

Now we have the tools to calculate the induced electric field in a pipeline and to determine the pipe-to-soil potentials produced by that electric field. In the following section, these tools will be used to examine how the soil resistivity influences the AC interference to a pipeline.

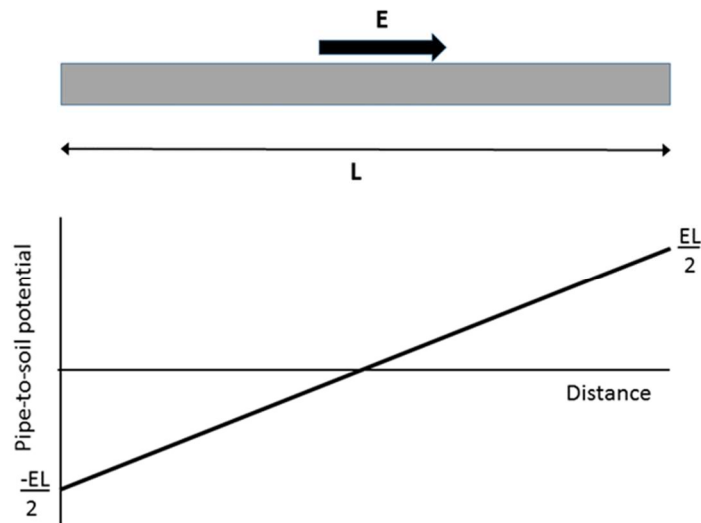


Figure 4 Pipeline of length L subjected to an induced electric field, E

Example Calculations: Uniform soil model

Figure 5 shows the layout of a pipeline adjacent to a 3-phase power line. The pipeline is assumed to be in a uniform soil model, with no Cathodic Protection (CP) and with no earthing systems attached to it. That is, the pipeline is assumed to be floating with respect to earth.

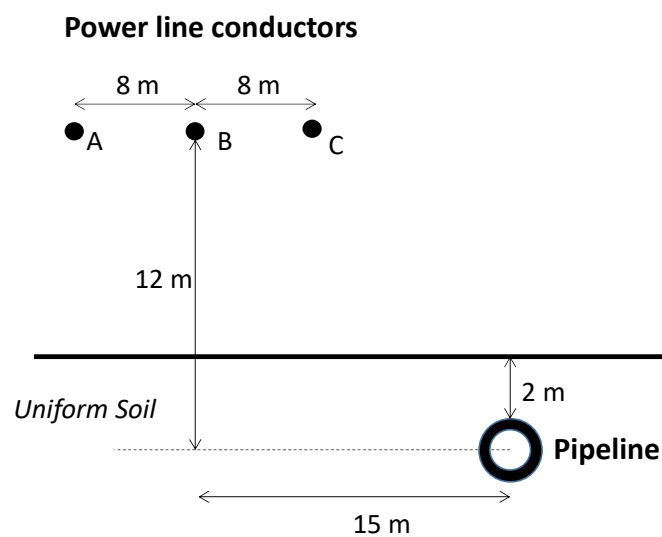


Figure 5 Pipeline adjacent to a 3-phase power line – uniform soil conditions

Table 1 summarises the important characteristics and parameters of the system shown in Figure 5.

Table 1 Input parameters

Height of conductor from centre of pipe (m)	h=12 m
Distance between phase A and B (m)	d ₁ =8 m
Distance between phase B and C (m)	d ₂ =8 m
Distance from centre of pipe to phase B (m)	d ₃ =15 m
Top of pipeline below surface (m)	d ₄ =2 m
Coating conductance	5 μS.m ⁻²
Pipe diameter	1 m
Pipe wall thickness	10 mm
Pipeline length	5 km
Uniform soil resistivity, ρ	100 Ω.m
Current Magnitude (A) for phase A, I _a	500 A
Current Magnitude (A) for phase B, I _b	500 A
Current Magnitude (A) for phase C, I _c	500 A
Current angle (degrees) for phase A	0 °
Current angle (degrees) for phase B	-120 °
Current angle (degrees) for phase C	-240 °
Frequency, f	50 Hz

Calculations for Normal Operating Conditions using Carson-Clem Expression

The mutual impedance is given by the expression from Carson-Clem as in (22).

$$Z_m = \frac{\mu_0 \cdot \omega}{8} + j\mu_0 \cdot f \cdot \ln \frac{1.85}{\alpha \cdot D} \quad (\Omega/m) \quad (22)$$

Where,

- $\mu_0 = 4\pi \times 10^{-7}$ (H/m)
- f is the frequency (Hz)
- $\alpha = \sqrt{\frac{\mu_0 \cdot \omega}{\rho}}$
- ρ is the soil resistivity (Ω/m)
- D is the geometrical distance between conductors

Thus, Z_{ap} , Z_{bp} , and Z_{cp} are defined in (23), (24) and (25):

$$Z_{ap} = \frac{\mu_0 \cdot \omega}{8} + j\mu_0 \cdot f \cdot \ln \frac{D_{ep}}{D_{ap}} \quad (\Omega/m) \quad (23)$$

$$Z_{bp} = \frac{\mu_0 \cdot \omega}{8} + j\mu_0 \cdot f \cdot \ln \frac{D_{ep}}{D_{bp}} \quad (\Omega/m) \quad (24)$$

$$Z_{cp} = \frac{\mu_0 \cdot \omega}{8} + j\mu_0 \cdot f \cdot \ln \frac{D_{ep}}{D_{cp}} \quad (\Omega/m) \quad (25)$$

Where,

$$D_{ep} = 658.37 \times \sqrt{\frac{\rho}{f}} \quad (m) \quad (26)$$

Table 2 Calculation of distances

$D_{ap} = \sqrt{h^2 + (d_1 + d_2)^2}$	25.942 m
$D_{bp} = \sqrt{h^2 + d_3^2}$	19.209 m
$D_{cp} = \sqrt{h^2 + (d_3 - d_2)^2}$	13.892 m
$D_{ep} = 658.37 \times \sqrt{\frac{\rho}{f}}$	931.076 m

Table 3 Calculation of mutual impedances

$Z_{ap} = \frac{\mu_0 \cdot \omega}{8} + j\mu_0 \cdot f \cdot \ln \frac{D_{ep}}{D_{ap}}$	4.9348e-05 + 2.2497e-01 j Ω/km 0.225 \angle 89.987 $^\circ$ Ω/km
$Z_{bp} = \frac{\mu_0 \cdot \omega}{8} + j\mu_0 \cdot f \cdot \ln \frac{D_{ep}}{D_{bp}}$	4.9348e-05 + 2.4385e-01 j Ω/km 0.244 \angle 89.988 $^\circ$ Ω/km
$Z_{cp} = \frac{\mu_0 \cdot \omega}{8} + j\mu_0 \cdot f \cdot \ln \frac{D_{ep}}{D_{cp}}$	4.9348e-05 + 2.6421e-01 j Ω/km 0.264 \angle 89.990 $^\circ$ Ω/km

The resultant induced voltage, V_p , can be expressed in equation form as follows:

$$V_p = I_a \times Z_{ap} + I_b \times Z_{bp} + I_c \times Z_{cp} \quad (V) \quad (27)$$

Where:

- I_a, I_b and I_c are the vector phase currents
- Z_{ap}, Z_{bp} , and Z_{cp} are the mutual impedances between the respective a, b and phase conductors and the pipeline

Thus, V_p is calculated as 8.8165 - 14.529 j V/km for a uniform 100 Ωm soil resistivity. For a 5 km floating pipeline the induced voltage in polar format will appear as $\pm 42.489\angle -58.75^\circ$ V

Calculations for Normal Operating Conditions using Complex Image Method

To use the complex image method to calculate the AC induction into the pipeline we need to consider the currents in the three individual phase conductors as well as the image current for each one as illustrated in Figure 6 where:

- D_{ap}, D_{bp} and D_{cp} are the distances from the pipeline to each power line conductor
- D_{ai}, D_{bi} and D_{ci} are the distances from the pipeline to the image of each power line conductor
- h is the height of conductor from the centre of pipe
- p is complex skin depth

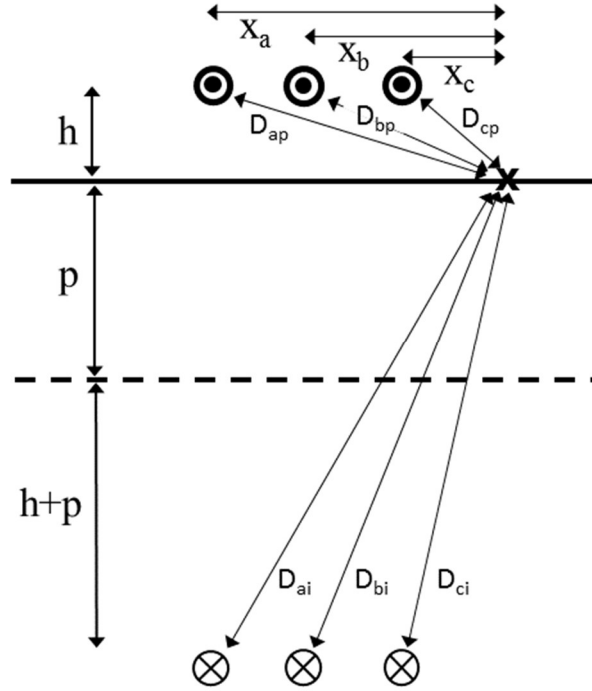


Figure 6 Three- phase currents and their image currents

For the power line shown in Figure 6 and the parameters in Table 1, the distances needed for the complex image calculations are given in Table 4;

Table 4 Calculation of distances from pipeline

$D_{ap} = \sqrt{h^2 + x_a^2}$	25.942 m
$D_{bp} = \sqrt{h^2 + x_b^2}$	19.209 m
$D_{cp} = \sqrt{h^2 + x_c^2}$	13.892 m
$p = \left(\frac{\rho}{j2\pi f \mu_0} \right)^{0.5}$	355.88 - 355.88 j
$D_{ai} = \sqrt{(h + 2p)^2 + x_a^2}$	723.95 - 711.58 j
$D_{bi} = \sqrt{(h + 2p)^2 + x_b^2}$	723.84 - 711.68 j
$D_{ci} = \sqrt{(h + 2p)^2 + x_c^2}$	723.78 - 711.746 j

For induction in the pipeline from a 3-phase power line the calculation of equation (3) needs to be repeated 3 times, once for each phase conductor, and the results added together. Thus, the electric field produced by AC from a 3-phase power line can be written as in (28).

$$E = jf\mu_0 \left\{ \ln \left[\frac{D_{ai}}{D_{ap}} \right] I_a + \ln \left[\frac{D_{bi}}{D_{bp}} \right] I_b + \ln \left[\frac{D_{ci}}{D_{cp}} \right] I_c \right\} \quad (28)$$

However, from [12], noting that $\ln \left[\frac{a}{b} \right] = \ln \left[\frac{1}{b} \right] - \ln \left[\frac{1}{a} \right]$, we can write equation (28) in the form:

$$E = jf\mu_0 \left\{ \ln \left[\frac{1}{D_{ap}} \right] I_a + \ln \left[\frac{1}{D_{bp}} \right] I_b + \ln \left[\frac{1}{D_{cp}} \right] I_c \right\} - jf\mu_0 \left\{ \ln \left[\frac{1}{D_{ai}} \right] I_a + \ln \left[\frac{1}{D_{bi}} \right] I_b + \ln \left[\frac{1}{D_{ci}} \right] I_c \right\} \quad (29)$$

This can be written in the form

$$E = jf\mu_0 \{ a_p I_a + b_p I_b + c_p I_c \} - jf\mu_0 \{ a_i I_a + b_i I_b + c_i I_c \} \quad (30)$$

Where the coefficients a_p , a_i , etc. in (30) are the scaling factors for each current due to their distance away from the pipeline. The calculation of these coefficients for 100 $\Omega.m$ is summarised in Table 5.

Table 5 Calculation of coefficients for 100 $\Omega.m$ homogeneous soil resistivity

a_p	-3.256
b_p	-2.955
c_p	-2.631
a_i	-6.9227516799714 + 0.77678239872057 j
b_i	-6.9227491600414 + 0.77692988634987 j
c_i	-6.9227477210136 + 0.77701527459999 j

Now we have all the parameters to calculate the electric field in the pipeline. Combining the scaling coefficients from Table 5 with the current magnitudes and phases from Table 1 and inserting in equation (30) gives the calculated electric field, E as $-8.8224 -14.5275 j \text{ V.km}^{-1}$ for a uniform 100 $\Omega.m$ soil resistivity. For a 5 km floating pipeline the induced voltage will appear in polar format as $\pm 42.49 \text{ V}$ with a phase angle -121.27° .

The same calculation procedure can be repeated for different values of uniform soil resistivity. The results are shown in Table 6.

Table 6 Calculation of pipe-to-soil potentials with different soil resistivities

Soil resistivity	E (phasor) - (V/km)	E (magnitude) - (V) @ 5 km
10 $\Omega.m$	-8.8728 -14.5044 j	± 42.5076
100 $\Omega.m$	-8.8224 -14.5275 j	± 42.4914
1000 $\Omega.m$	-8.8171 -14.5297 j	± 42.4892

The results from the complex image method explained above have been compared to results obtained using Carson's equations and the results produced by a CDEGS equivalent model. (Table 7). This shows the validity of the complex image method. However, the significant result shown in Table 6 and Table 7 is that the pipe-to-soil potential produced by 3-phase 50 Hz AC is independent of the value used for soil resistivity.

Table 7 Comparison of AC pipe-to-soil potentials obtained with different calculation methods

	Complex Image Method	Carson 's equations	CDEGS calculations
10 Ωm	± 42.5076	± 42.5709	± 42.25309
100 Ωm	± 42.4914	± 42.5083	± 43.03546
1000 Ωm	± 42.4892	± 42.4994	± 42.7578

Example Calculation: Two-layer soil model

Figure 7 shows the layout of a pipeline adjacent to a 3-phase power line. The pipeline is assumed to be in a surface layer, 5 m thick, with soil resistivity, $\rho_1=\rho_S$. Underneath is a deeper layer extending to infinite depth, with resistivity, $\rho_2=\rho_D$. As for the uniform soil calculations, the pipeline has no Cathodic Protection (CP) and no earthing systems attached to it, so it is assumed to be floating with respect to earth.

To do the calculations in this case, we need to use equations (7) and (11) to calculate the surface impedance, Z_S . This is then used in equation (4) to calculate the complex skin depth, p , which is then used, as before, to calculate the distances needed for the complex image calculations.

The input parameters are shown in Table 8 and Table 9 shows the results of the calculations.

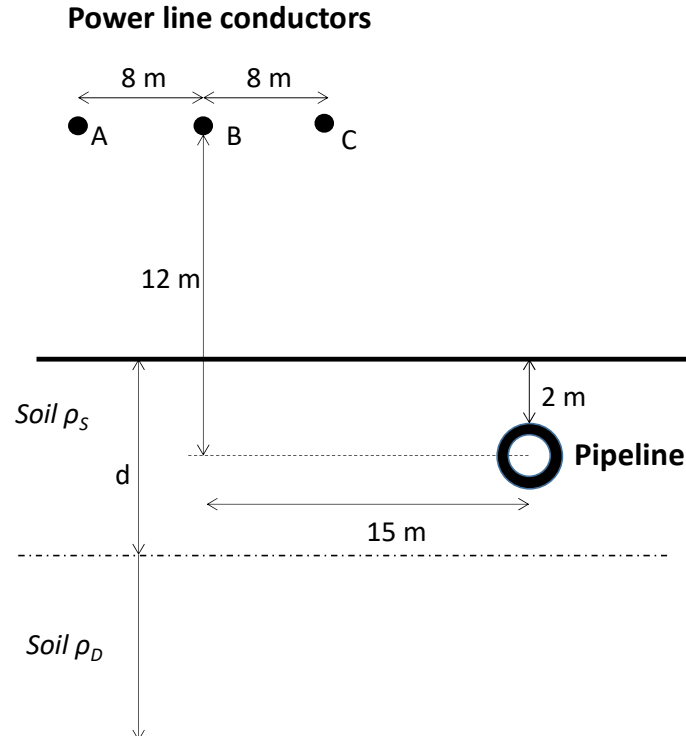


Figure 7 Pipeline adjacent to a 3-phase power line – Horizontal two-layer soil conditions

Table 8 Input parameters for horizontal two-layer soil conditions

Height of conductor from centre of pipe (m)	h=12 m
Distance between phase A and B (m)	d ₁ =8 m
Distance between phase B and C (m)	d ₂ =8 m
Distance from centre of pipe to phase B (m)	d ₃ =15 m
Top of pipeline below surface (m)	d ₄ =2 m
Coating conductance	5 μS.m ⁻²
Pipe diameter	1 m
Pipe wall thickness	10 mm
Pipeline length	5 km
soil resistivity of upper layer, ρ _S (thickness d=5m)	10 Ω.m
soil resistivity of deep layer, ρ _D (extending to infinite depth)	1000 Ω.m
Current Magnitude (A) for phase A	500 A
Current Magnitude (A) for phase B	500 A
Current Magnitude (A) for phase C	500 A
Current angle (degrees) for phase A	0 °
Current angle (degrees) for phase B	-120 °
Current angle (degrees) for phase C	-240 °
Frequency, f	50 Hz

Table 9 Calculation results

$Z_D = \sqrt{i2\pi f \mu_0 \rho_D}$	0.4443 + 0.4443 j
$Z_0 = \sqrt{i2\pi f \mu_0 \rho_S}$	0.04442882938 + 0.04442882938 j
$R = \frac{Z_0 - Z_D}{Z_0 + Z_D}$	-0.8182
$k = \sqrt{\frac{i2\pi f \mu_0}{\rho_S}}$	0.00444288293815 + 0.00444288293815 j
$Z_S = Z_0 \left(\frac{1 - Re^{-2kd}}{1 + Re^{-2kd}} \right)$	0.416114858445084 + 0.289519045183952 j
$p_2 = \frac{Z_S}{i2\pi f \mu_0} = \sqrt{\frac{\rho_S}{i2\pi f \mu_0}} \left(\frac{1 - Re^{-2kd}}{1 + Re^{-2kd}} \right)$	733.360308625938 - 1054.03124972049 j
$D_{ap} = \sqrt{h^2 + x_a^2}$	25.942 m
$D_{bp} = \sqrt{h^2 + x_b^2}$	19.209 m
$D_{cp} = \sqrt{h^2 + x_c^2}$	13.892 m
$D_{ai} = \sqrt{(h + 2p_2)^2 + x_a^2}$	1478.77960710615 - 2107.97840692371 j
$D_{bi} = \sqrt{(h + 2p_2)^2 + x_b^2}$	1478.74570697116 - 2108.02673217140 j
$D_{ci} = \sqrt{(h + 2p_2)^2 + x_c^2}$	1478.72608117424 - 2108.05471010800i

Now we have all the parameters to calculate the electric field in the pipeline. Combining the parameters from Table 9 with the current magnitudes and phases from Table 8 gives the calculated electric field, E as -8.8175 -14.5299 j V/km for a horizontal two-layer soil model

(10 / 1000 $\Omega\cdot\text{m}$). For a 5 km floating pipeline the induced voltage will appear as $\pm 42.4901 \text{ V}$ – phase angle -121.25° .

The same calculation procedure can be repeated for different values of surface resistivity and deep resistivity. For comparison, calculations were made for a 2-layer earth model with a surface layer with a resistivity of 1000 ohm-m above a deeper layer with resistivity of 10 ohm-m (see Table 10). This also shows results produced by a CDEGS equivalent model

Table 10 Comparison of pipe-to-soil potentials from different calculation methods – for horizontal two-layer soil

	Complex Image Method	CDEGS calculations
Upper 10 Ωm / Deep 1000 Ωm	$\pm 42.4901 \text{ V}$	$\pm 42.65803 \text{ V}$
Upper 1000 Ωm / Deep 10 Ωm	$\pm 42.5008 \text{ V}$	$\pm 42.33028 \text{ V}$

These results show that the pipe-to-soil potential is not affected by changing the resistivity of the layers within a 2-layer earth model. Comparison of the results in Table 10 with those in Table 6 shows that the same pipe-to-soil potential values are being obtained in all cases, further showing that the pipe-to-soil potential produced by 3-phase 50 Hz AC is independent of the values used for soil resistivity.

Discussion

The above results showing that AC interference in a pipeline is independent of the soil resistivity may appear surprising.

Other calculations of electromagnetic induction in the earth, across a range of frequencies, all show a dependence on the resistivity with the skin depth being a critical parameter used. The skin depth shows the distance for the fields to reduce to 0.37 (1/e) of their value at the surface and is used as an indicator of the depths for which resistivity values are needed. The skin depth is dependent on both frequency and soil resistivity. Figure 8 shows the skin depth at a frequency of 50 Hz for a range of soil resistivity values and clearly shows that the skin depth increases for higher values of soil resistivity.

However, the major difference about AC induction is that the source is a set of 3-phase currents, whereas other studies involve ‘plane wave’ or single conductor sources. The 3-phase nature of the AC currents seems to have been overlooked in the past when thinking about AC interference problems.

Calculations using Carson’s equations can be complicated. However, using the complex image method simplifies the calculations and makes it easier to visualise the contributions from different sources. The key feature of the complex image method is that the fields produced at the surface by currents induced in the Earth can be represented by the fields produced by an image current at a complex depth, $h+2p$ where p is the complex skin depth. For AC interference from a 3-phase power line, we have shown that there are 3 image currents that must be included in the calculations.

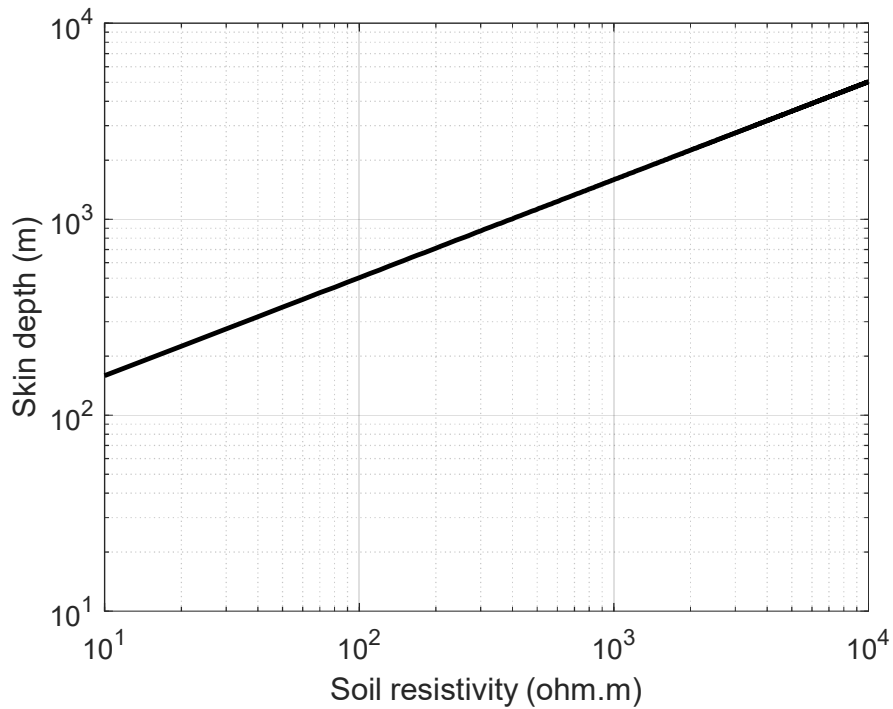


Figure 8 Dependence of skin depth on soil resistivity.

The calculations for the complex image method make use of the distances from the pipeline to each of the 3 conductors that make up a 3-phase power line, as well as the distances to the 3 image currents. Consider first the power line currents. These are 120° out of phase with each other and where these currents come together in the power system (for example, at the neutral point of a Y-connected transformer) they sum to zero. Similarly, at a point equidistant from the 3 currents, the magnetic fields and induced electric fields they produce would also sum to zero. It is only because the power lines are at different distances from the pipeline that the interference from the currents in each power line do not cancel out at the pipeline.

Now consider the image currents. These are also 120° out of phase with each other (although they do not have the same phases as the power line currents). Thus the magnetic and induced electric fields produced by the image currents also tend to cancel out. How effectively they do this depends on the differences in their distances from each image current to the pipeline. The calculation of the distance from the image current to the pipeline is shown in Figure 1 and depends on the horizontal distance, x , from the image current to the pipeline, and the depth of the image current, $h+2p$. The soil resistivity affects the value of p , so this would appear to indicate how the soil resistivity influences the results of the calculations.

However, it is necessary to take account of the fact that there are 3 image currents as shown in Figure 6. The distances to the pipeline are all slightly different; the differences coming from the different values for the horizontal distance, x . How much of an effect these differences in x have on the absolute distances D_{ai} , D_{bi} and D_{ci} depend on the relative sizes of the vertical distance, $h+2p$, and the horizontal distance, x . For a soil resistivity of 100 ohm-m, and frequency of 50 Hz, the skin depth is about 500 m, giving a vertical distance, $h+2p$, equal to 1012 m. This is much greater than the horizontal distances to the pipeline, 7 m, 15 m, and 23 m. Thus, there is not much difference in complex values for D_{ai} , D_{bi} and D_{ci} (as shown in

Table 2). Because of this, the contributions from the three image currents to the fields at the pipeline almost sum to zero.

The same estimates can be made for a soil resistivity of 1000 ohm-m. In this case the skin depth is approximately 1580 m, so the vertical distance, $h+2p$, will be 3172 m. Now the differences in the horizontal distances will make an even smaller difference in the complex values for D_{ai} , D_{bi} and D_{ci} . This is shown by the values in Table 9 which are for a 2-layer earth, but it is obvious that with the skin depths involved the waves have penetrated through the surface layer and the response is dominated by the deeper layer which has a resistivity of 1000 ohm-m. Because the distances from the pipeline to the image currents are more nearly the same, compared to the 100 ohm.m values, then the fields from the 3 image currents will more closely sum to zero at the pipeline.

Figure 9 shows the relative size of the contributions to the induced electric field in the pipeline from the power line currents and from the image currents. This shows that, as the resistivity increases the image currents get deeper, so their distances to the pipeline become relatively closer with the results that fields from the image currents, that are 120° out of phase with each other, more nearly cancel each other, so make a smaller contribution. Figure 9 also shows that over all of the range of soil resistivity values that are normally encountered, the contributions from the image currents are much smaller than the contributions from the power line currents. Thus, the calculation of the AC interference to the pipeline is not affected by the depth to the image currents, so the soil resistivity has no influence on the results.

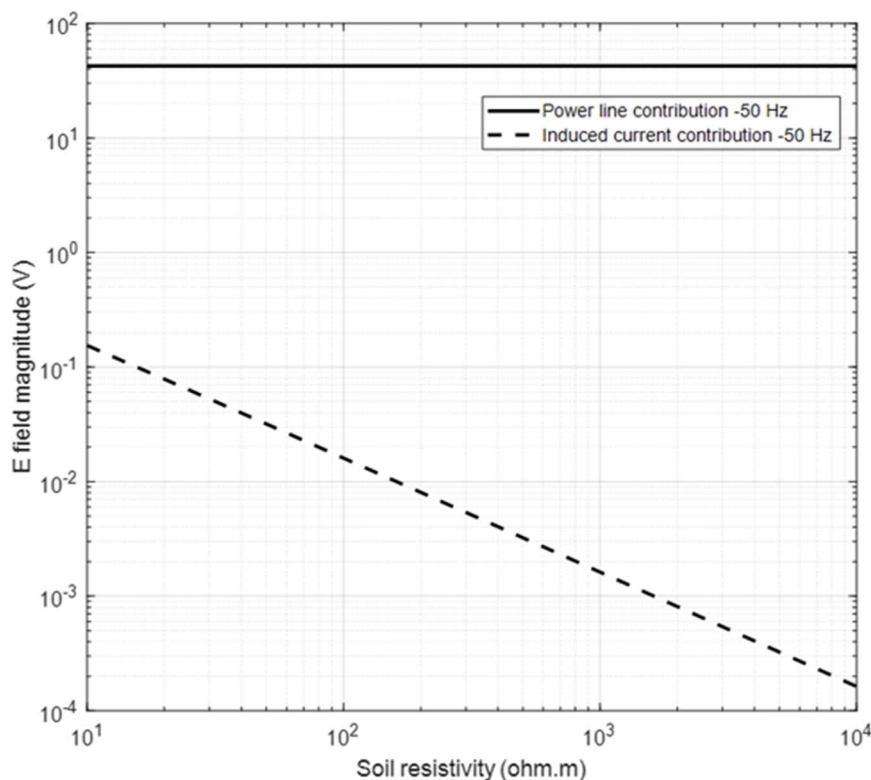


Figure 9 The contributions to the electric field in the pipeline from power line currents at the fundamental frequency (50 Hz) and induced currents in the earth, including the dependence of the latter on soil resistivity.

Conclusions

It has been shown how to model AC induction into a pipeline, including possible effects of induced currents in the earth, using the complex image method. This, combined with a pipeline model can be used to determine the pipe-to-soil potential variations produced by AC interference.

Example calculations are presented to show how to calculate AC interference from 3-phase 50 Hz power line currents, using a uniform soil resistivity model and a 2-layer resistivity model. All the calculations give the same result, independent of the value used for soil resistivity.

This is explained by the 3-phase nature of the source currents in the power line. These produce image currents in the earth that are also 120° out of phase with each other so that the fields they produce at the pipeline tend to sum to zero. For all expected values of soil resistivity, the contributions to the electric fields in the pipeline from the image currents are much less than the contributions from the power line currents. Thus, the depth to the image currents, which is how soil resistivity enters the calculation, has virtually no effect on the results.

These results show that the soil resistivity has no material effect on the calculation of induced AC pipe-to-soil potentials in the pipeline, which are used as part of the assessment for the risk of external corrosion. Deep soil resistivity measurements are not required to determine the levels of induced voltage, under steady-state operating conditions of a power line.

References

- [1] CEN, *EN 12501-2 Protection of metallic materials against corrosion - Corrosion likelihood in soil*, CEN, 2003.
- [2] ISO, "15589-1 Petroleum and Natural gas industries - cathodic protection of pipeline transportation systems - Part 1 On land pipelines," ISO.
- [3] ISO, "18086 Corrosion of materials and alloys - determination of ac corrosion - protection criteria," ISO.
- [4] ISO, *ISO 21857 Petroleum, petrochemical and natural gas industries - Prevention of corrosion on pipeline systems influenced by stray currents*, ISO.
- [5] ASTM, *ASTM G 57 Standard test method for field measurement of soil resistivity using Wenner four-electrode method*, ASTM, 2012.
- [6] J. R. Carson, "Wave propagation on over-head wires with ground return," *Bell System Technical Journal*, vol. 5, pp. 539-554, 1926.
- [7] AS/NZS, *Electrical Hazards on metallic pipelines*, AS/NZS, 2012.
- [8] CIGRE, "Guide on the influences of high voltage AC power systems on metallic pipelines," CIGRE, 1995.
- [9] A. Deri and G. Tevan, "Mathematical verification of Dubanton's simplified calculation of overhead transmission line parameters and its physocal interpretation," *Archiv fur Elektrotechnik* 63, pp. 191-198, 1981.
- [10] D. H. Boteler and L. Trichtchenko, "A Common Theoretical Framework for AC and Telluric Interference on Pipelines, Paper No 05614," in *CORROSION/2005*, Houston, 2005.
- [11] A. Deri, G. Tevan, A. Castanheira and A. Semlyen, "The complex ground return plane A simplified model for homogeneous and multi-layer earth return.," *IEEE Transactions on Power Apparatus and Systems*, Vols. PAS-100, No 8, 1981.
- [12] D. H. Boteler, C. A. Charalambous and K. C. Lax, "New Insights into Calculations of AC Interference at Fundamental and Harmonic Frequencies taking account of the phase relationships of the currents" *IEEE Trans. Power Delivery*, Submitted 2020.
- [13] D. Boteler, "Distributed-source transmission line theory for electromagnetic induction studies," in *Zurich EMC composium*, Zurich, 1997.
- [14] A. Taflove and J. Dabkowski, "Prediction method for buried pipeline voltages due to 60 Hz AC inductive coupling," *IEEE Trans. Power Apparatus & Systems*, Vols. PAS-98, pp. 780-794, 1979.

Appendix: Complex Skin Depth for a Uniform and Layered Earth

Starting with Maxwell's equations in the derivative form and noting that, for the earth resistivities, ρ , and frequencies, f , we are concerned with for AC interference, the displacement current term is negligible, the relationships between magnetic field, \mathbf{H} , and electric field, \mathbf{E} , can be written

$$\nabla \times \mathbf{E} = -j2\pi f \mu_0 \mathbf{H} \quad (\text{A.1})$$

$$\nabla \times \mathbf{H} = \frac{1}{\rho} \mathbf{E} \quad (\text{A.2})$$

Where μ_0 is the magnetic permeability of free space which has a value of $4\pi \cdot 10^{-7}$ H/m. Taking the curl of (A.1) and substituting into (A.2) gives the diffusion equation

$$\nabla^2 \mathbf{E} = \frac{j2\pi f \mu_0}{\rho} \mathbf{E} \quad (\text{A.3})$$

The response of the earth is usually expressed in terms of a plane wave travelling vertically down into the earth. If the earth is assumed to be a uniform half-space with resistivity, ρ , equation (A.3) has a solution of the form

$$\mathbf{E} = E_0 e^{-kz} \quad (\text{A.4})$$

where E_0 is the amplitude of the electric field at the Earth's surface, z is the distance below the surface, and k is the propagation constant given by

$$k = \sqrt{\frac{j2\pi f \mu_0}{\rho}} \quad (\text{A.5})$$

Substituting \mathbf{E} from (A.4) back into equation (A.1) gives the surface impedance of the earth relating the orthogonal surface electric and magnetic fields

$$Z_S = -\frac{E_0}{H_0} = \sqrt{j2\pi f \mu_0 \rho} \quad (\text{A.6})$$

The complex skin depth, p , is related to the surface impedance, Z_S , by

$$p = \frac{Z_S}{j2\pi f \mu_0} \quad (\text{A.7})$$

For a uniform resistivity this gives

$$p = \sqrt{\frac{\rho}{j2\pi f \mu_0}} \quad (\text{A.8})$$

In practice the earth resistivity varies with depth. This can be modelled by representing the earth as a set of layers of specified resistivity and depth, with layer 1 at the surface, layer 2 underneath that, and so on.. Consider a single layer, n , of thickness d_n with resistivity ρ_n within this model. The fields at the top surface of layer n are E_n and H_n as shown in Figure A.1.

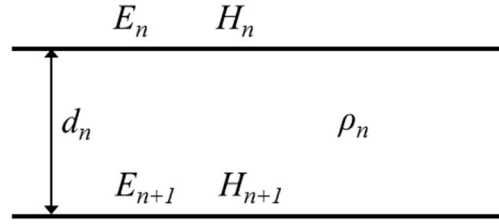


Fig. A.1. Electric and magnetic fields at the top and bottom surfaces of a layer.

At the bottom of the layer, because of continuity of the tangential fields across a boundary, the fields are the same as the fields at the top of the underlying layer, $n+1$, so can be written E_{n+1} and H_{n+1} . Within this layer, equation (A.3) still applies but the solution is now given by a combination of a downward travelling wave (the same as in (A.4)), and an upward travelling wave produced by reflection from the bottom boundary of the layer.

$$E = A_n e^{-kz} + B_n e^{kz} \quad (\text{A.9})$$

$$H = \frac{A_n}{\eta_n} e^{-kz} - \frac{B_n}{\eta_n} e^{kz} \quad (\text{A.10})$$

Where A_n and B_n are the amplitudes of the electric field downward and upward travelling waves at the top surface of the layer, k_n is the propagation constant within the layer

$$k_n = \sqrt{\frac{i2\pi f \mu_0}{\rho_n}} \quad (\text{A.11})$$

and η_n is the characteristic impedance of the layer

$$\eta_n = \sqrt{j2\pi f \mu_0 \rho_n} \quad (\text{A.12})$$

Combining equations (A.9) and (A.10) with $z=0$ gives the ratio of the fields at the top surface of the layer

$$Z_n = - \frac{E_n}{H_n} = \left(\frac{1+B/A}{1-B/A} \right) \eta_n \quad (\text{A.13})$$

Similarly the ratio of the fields at the bottom surface of the layer, with $z = d_n$, is given by

$$Z_{n+1} = - \frac{E_{n+1}}{H_{n+1}} = \left(\frac{A_n e^{-k_n d_n} + B_n e^{k_n d_n}}{A_n e^{-k_n d_n} - B_n e^{k_n d_n}} \right) \eta_n \quad (\text{A.14})$$

This represents the “terminating impedance” seen by the layer.

$A_n e^{-k_n d_n}$ and $B_n e^{k_n d_n}$ are the amplitudes, at the bottom surface of the layer, of the downward and upward travelling waves and are related by the reflection coefficient at the bottom surface

$$R_{n+1} = - \frac{B(d)}{A(d)} = \frac{B_n e^{k_n d_n}}{A_n e^{-k_n d_n}} \quad (\text{A.15})$$

So equation (A.14) can be written

$$Z_{n+1} = \left(\frac{1+R_{n+1}}{1-R_{n+1}} \right) \eta_n \quad (\text{A.16})$$

Rearranging this gives

$$R_{n+1} = \left(\frac{Z_{n+1}-\eta_n}{Z_{n+1}+\eta_n} \right) \quad (\text{A.17})$$

Thus, the reflection coefficient can be calculated from the characteristic impedance of the layer and the impedance at the top surface of the underlying layer. Now, rearranging (A.15), we can write

$$\frac{B_n}{A_n} = R_{n+1} e^{-2k_n d_n} \quad (\text{A.18})$$

which, substituted in (A.13) gives

$$Z_n = \left(\frac{1 + R_{n+1} e^{-2k_n d_n}}{1 - R_{n+1} e^{-2k_n d_n}} \right) \eta_n \quad (\text{A.19})$$

Now we can express the impedance at the top surface of the layer in terms of the characteristics of the layer and the reflection coefficient at the bottom surface of the layer. This gives us the means to calculate the surface impedance at the top of a layered model of the Earth. The bottom layer extends to infinite so can be treated as a uniform half-space, so the impedance at its surface is given by equation (A.6). This then appears as the terminating impedance for the next layer up and can be substituted into (A.17) along with the characteristic impedance of that layer to calculate the reflection coefficient at the bottom surface of the layer. Inserting this reflection coefficient, along with the layer properties, in (A.19) then gives the impedance at the top surface of the layer. This then appears as the terminating impedance for the next layer up and the same series of steps leads to the impedance at the top of that layer, and so on, up to the surface of the Earth, to give the surface impedance, Z_s . This can be substituted in (A.7) to give the complex skin depth for the layered model.